Available online at www.sciencedirect.com
ScienceDirect
Quaternary Research 66 (2006) 233 – 245
QUATERNARY RESEARCH
www.elsevier.com/locate/yqres

# Speleology and magnetobiostratigraphic chronology of the Buffalo Cave fossil site, Makapansgat, South Africa

Andy I.R. Herries [a,b,*], Kaye E. Reed [c], Kevin L. Kuykendall [d], Alf G. Latham [e]

[a] Geomagnetism Laboratory, University of Liverpool, L69 7ZE, UK
[b] Palaeoanthropology Research Group, School of Medical Sciences, University of New South Wales, Kensington, Sydney 2052, Australia
[c] Institute of Human Origins, Arizona State University, Tempe, AZ 85281, USA
[d] Department of Archaeology, University of Sheffield, UK
[e] Department of Archaeology, Hartley Building, University of Liverpool, L69 3BX, UK

Received 30 September 2004
Available online 12 June 2006

**Abstract**

Speleological, stratigraphic, paleomagnetic and faunal data is presented for the Buffalo Cave fossil site in the Limpopo Province of South Africa. Speleothems and clastic deposits were sampled for paleomagnetic and mineral magnetic analysis from the northern part of the site, where stratigraphic relationships could be more easily defined and a magnetostratigraphy could therefore be developed for the site. This is also where excavations recovered the fossil material described. A comparison of the east and South African first and last appearance data with the Buffalo Cave fauna was then used to constrain the magnetostratigraphy to produce a more secure age for the site. The magnetostratigraphy showed a change from normal to reversed polarity in the basal speleothems followed by a short normal polarity period in the base of the clastic deposits and a slow change to reversed directions for the remainder of the sequence. The biochronology suggested an optimal age range of between 1.0 Ma and 600,000 yr based on faunal correlation with eastern and southern Africa. A comparison of the magnetobiostratigraphy with the GPTS suggests that the sequence covers the time period from the Olduvai event between 1.95 and 1.78 Ma, through the Jaramillo event at 1.07 Ma to 990,000 yr, until the Bruhnes–Matuyama boundary at 780,000 yr. The faunal-bearing clastic deposits are thus dated between 1.07 Ma and 780,000 yr with the main faunal remains occurring in sediments dated to just after the end of the Jaramillo Event at 990,000 yr.


*Keywords:* Paleomagnetism; Jaramillo event; Biochronology; Late early Pleistocene fauna; Makapansgat; South Africa

## Introduction

Buffalo Cave (Figs. 1 and 2) is situated at the base of a 20-m cliff on the northern flank of the Zwartkrans Valley on the Makapansgat Farm, near Mokopane in the Limpopo Province (previously the Northern Transvaal) of South Africa. Although its exact age was unknown, the site was thought to provide a faunal assemblage intermediate in age between the nearby Plio-Pleistocene Makapansgat Limeworks site (ca. 4.19–2.16 Ma; Herries, 2003), bearing remains of *Australopithecus africanus*, and the middle to late Pleistocene Cave of Hearths (within the last 780,000 yr; Herries, 2003), bearing the remains of an archaic form of *Homo sapien* (*H.s. rhodesiensis*; Tobias, 1971). All three fossil sites occur on the Makapansgat Farm and together provide a long though discontinuous sequence of fossil deposits spanning approximately the past 4.0 Myr. Thus, as one of a series of sites in the Makapansgat Valley, the Buffalo Cave site has potentially great significance in providing information about long-term faunal and environmental evolutionary trends relevant to hominid evolution in southern Africa.

We have conducted intermittent fieldwork at Buffalo Cave since 1993, including recovery of fossils from both ex situ (dump and collapse deposits) and in situ provenance, and magnetostratigraphic sampling. A preliminary description of the faunal material recovered from ex situ lime miners dumps was presented by Kuykendall et al. (1995). The aim of this

* Corresponding author. Palaeoanthropology Research Group, School of Medical Sciences, University of New South Wales, Kensington, Sydney 2052, Australia.
*E-mail addresses:* andyherries@yahoo.co.uk (A.I.R. Herries), kreed.iho@asu.edu (K.E. Reed).

0033-5894/$ - see front matter © 2006 University of Washington. All rights reserved.
doi:10.1016/j.yqres.2006.03.006

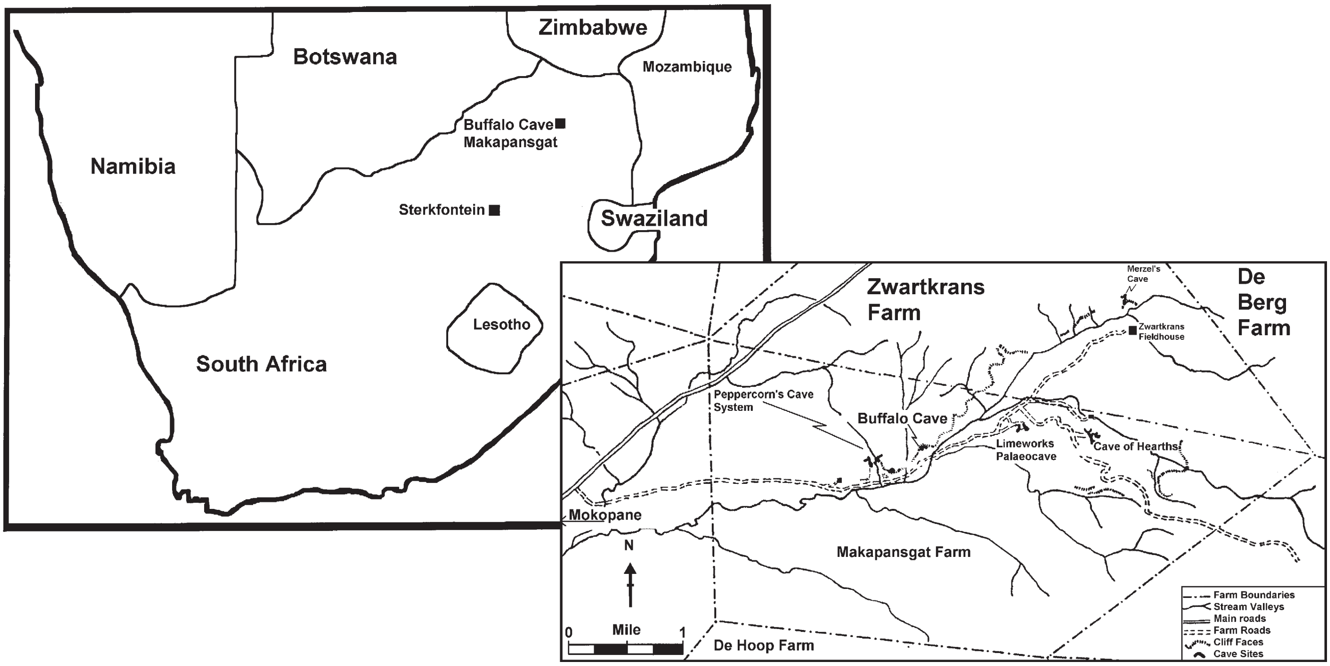


Figure 1. Location of Buffalo Cave, Makapansgat, Limpopo Province, South Africa and its relation to other fossil sites mentioned in the text (based on a map of Maguire, 1998).

paper is to present (a) a reconstruction of site formation processes at Buffalo Cave; (b) a magnetic polarity record and a chronology of those deposits based on a comparison of the site polarity record with the Geomagnetic Polarity Time Scale (GPTS; Ogg and Smith, 2004); and (c) to compare the magnetic chronology with age estimates based on the faunal assemblage recovered so far.

Like the well-known early hominid fossil localities in South Africa, Buffalo Cave was initially located because mining activity had exposed fossil breccias that attracted the attention of paleontologists and paleoanthropologists. Speleothem was mined at Buffalo Cave for the gold extraction process in the first half of the twentieth century. When it was active, the cave would have formed part of the underground drainage route for the northern side of the Zwartkrans Valley (Fig. 1). The main site is a remnant of an ancient, relict cave system that was almost entirely filled by speleothem and clastic sediments (Fig. 2). Mining and

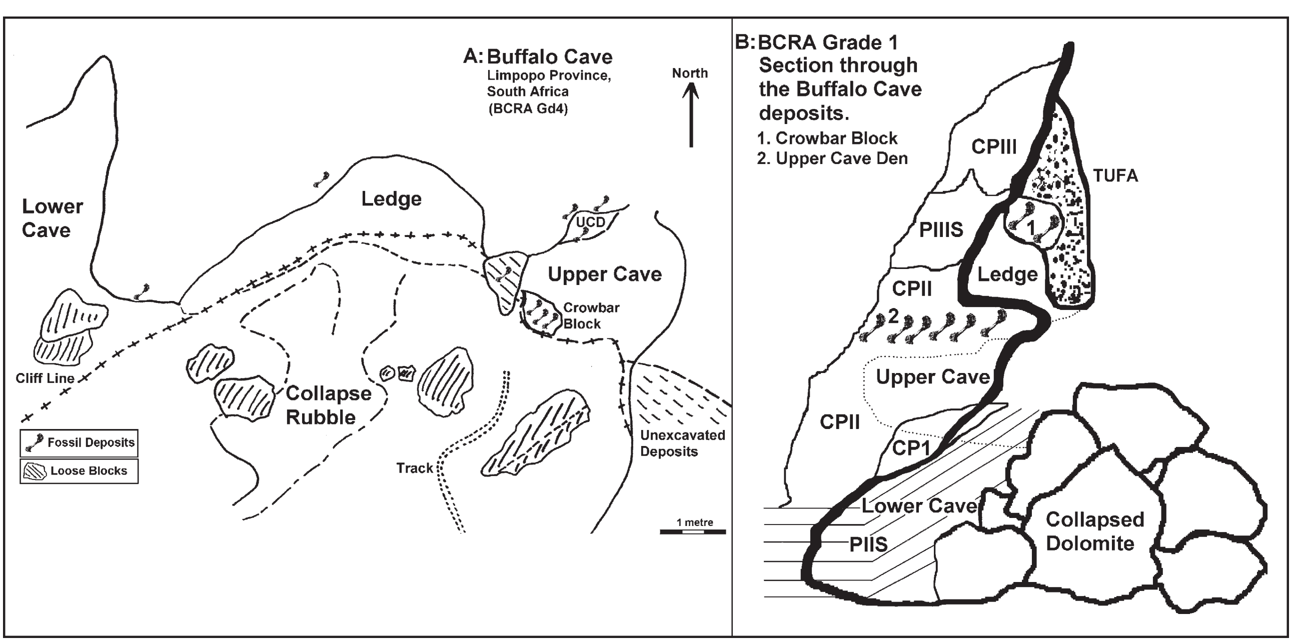


Figure 2. Survey of Buffalo Cave (A, plan; and B, north-south superimposed section) showing the main features as referred to in the text.

erosion has subsequently revealed most of these ancient infill deposits as section-like exposures. These consist of a series of paleodeposits consisting of speleothems, breccias, conglomerates and calcified sediments that in-filled the ancient cave system (here referred to as the paleocave so as to distinguish it from modern cavities), but the currently existing 'cave' site actually consists of excavated cavities resulting from extensive mining operations in the early part of the 20th century. Broom (1937–1948) recovered a small collection of fossils that were reported to have come from this site, in particular the remains of what he described as an extinct 'pygmy buffalo' (*Bos makapani*) after which the cave is named. Many other researchers visited the site over the years and recovered a small unprovenanced assemblage of fossil fauna that suggested a Pliocene to early Pleistocene age for the site, based on comparisons with similar east African fauna (Kuykendall et al., 1995). In Broom's original report (Broom, 1948), Buffalo Cave was described as being 'opposite the Limeworks,' but it is actually some 2 km down valley on the opposite ridge (Fig. 1), so there is some doubt about the exact find spot of the extinct buffalo remains (Tobias, 1997).

The mining activities left an excavated bowl in the hillside with three main subsurface chambers in which the paleodeposits are exposed and an extensive pile of collapse and rubble in the center of the site (Fig. 2). The more eastern upper chamber has been designated the upper cave (UC), and the more western lower chamber as the lower cave (LC). The southern part of the site consists of a series of relatively sterile and eroded breccias that outcrop and form part of the modern hillside. These deposits were not associated with large amounts of speleothem and were tunneled through and only partly undercut by mining activities. Untouched cave fills also occur to the east of the upper cave. Over much of the site, mining and subsequent collapse has since obscured the stratigraphic relationships of some deposits, particularly the relationship of the southern collapse breccias and the faunal-bearing northern deposits studied in this paper. Moreover, the site receives a carbonate-rich surface flow from higher up the existing cliff that has resulted in the re-deposition of clastic material and of a 10-m-wide, 20-m-long drapery of a moss- and fern-rich tufa that now obscures part of the western site and has added to the stratigraphic complexity.

The faunal material recovered during excavation all derive from the upper cave deposits, but additional extensive deposits occur higher in the stratigraphy and beneath the more recent tufa (for example, the Crowbar Block; Figs. 2 and 3). Evidently, one or more grottos or clefts occupied this north western area of the ancient cave and were utilized by carnivores as primary denning sites. More than 90% of the bones so far recovered are of bovids and there is a good representation of hyena bones and coprolites, suggesting that the assemblage was deposited as a result of primary hyena denning. This deposit has been designated as the upper cave den (UCD). Some remains have been minimally redistributed by water in the upper cave fossil-bearing layers, as suggested by a decreasing distribution of bones away from the main accumulation throughout the upper cave fossil layers.

Figure 3. Density of fossils in part of the Crowbar Block.

## Speleology and stratigraphy

### *Introduction*

The Zwartkrans Valley (Fig. 1) is a graben formed between two sets of subparallel faults. The Buffalo paleocave was formed along part of the northern echelon fault zone of this graben. Slickensides on an exposed sidewall of Buffalo Cave provide evidence that the cave is situated on a fault zone. Other relict cave passages appear to lie across the zone, as do parts of other more modern caves on this side of the valley. These caves include the large hydrologically linked Peppercorns'–Katzenjammer–Ficus–Cold Air–Two Skulls Cave system down valley and Merzl's Cave close to the head of the valley (Fig. 1). Fossil-bearing paleocave deposits also occur here in the entrance to Katzemjammer Cave, also known as Stinkblaargat and in the entrance to Peppercorns' Cave. These caves formed by the enlargement of elements of the northern fault zone that acted as connected conduits for groundwater passing from the head of the valley out toward the Dorps River (Dorpspruit).

The northern 20 m stratigraphic sequence appears to run relatively uninterrupted from massive flowstone-covered dolomite blocks at its base to breccia remnants on the side of the cliff face. The basal deposits and floor rock remain in the most part subsurface and are not visible, except in one case in the upper cave. Although there are crosscutting surfaces between the much later tufa and other deposits, no erosional surfaces have been noted in this sequence. However, erosional surfaces are noted on the eastern side of the site where a heavily eroded basal flowstone underlies a block breccia deposit. Extensive erosional surfaces also occur across the site and are related to the erosion of the paleocave deposits since the complete infilling of the ancient cave and retreat of the cliff face. Erosion has obscured attempts to correlate the main northern fossil deposits with eastern and southern parts of the site.

Large, fossiliferous blocks detached from the top of the northern sequence during mining activities lie in the central portion of the mined cavity. Their stratigraphic placement can only be approximately reconstructed due to the extent to which mining, collapse, and the tufa have obscured stratigraphic relationships. This paper therefore concentrates on the identification of the strata and chronology of the northern fossil-rich deposits that remain in situ and are largely undisturbed.

Throughout the following section, references are made to the historically mined 'upper cave' and 'lower cave' (Fig. 2), as this makes a convenient division of the deposits and defines where they are exposed. However, the exposed deposits of both the upper and lower cave represent the infill of a single large rift, which during its lifetime may have had a more complicated structure. The oldest speleothem deposits are laid down on a steep slope and are exposed in both the upper and lower cave. The following stratigraphy, simplified from Herries (2003), forms the basis for the paleomagnetic sampling and a simplified section is shown in Figures 2b and 6.

*Basal phases I (PIS) and II (PIIS) speleothem*

The site as a whole appears to represent the collapse of the outer wall of a cavity that ran subparallel to the valley together with remnants of passages on complementary faults. Initial enlargement of the cavity took place due to percolating groundwater exploiting the fault cavity and due to collapse of the steep hillside that would eventually cause the creation of a lateral, although inclined, entrance to the surface. Upon abandonment, seepage water from the surface began to deposit speleothems in the ancient cave. These first deposits can be seen in the upper cave (UC), where large vertical flowstone curtains or 'draperies' hang down into an extensive area of rimstone dams, or 'gour pools,' that formed on the edge of a large collapsed dolomite block. This is termed phase I speleothem (PIS). The PIS was followed by massive subaerial flowstone deposits up to 3 m thick, termed phase II speleothem (PIIS), so that the lower parts of the PIS curtains eventually became enveloped in PIIS flowstone. The draperies appear to have caused a barrier around which the flowstone formed and this, in turn, created a small grotto between the draperies and the dolomite at the back of the cave. It was this cavity that was later exploited by carnivores as a den (the UCD), and it forms one of the two areas of dense bone accumulation within the cave.

As the massive PIIS accumulated down slope it built up and flattened out towards the rear of the cave and resulted in a 3-m deep section of flowstone. The flowstone sequence in the lower cave is broken 0.42 cm from its surface contact with the overlying clastic deposits. This break represents a hiatus in deposition and is associated with the presence of a thin layer of the mineral collophane, normally an indication of mineralized guano. A similar collophane crusts occur in the very top portion of the PIIS at the contact with the overlying clastic deposits. This suggests a series of hiatuses in deposition towards the end of the PIIS and before the deposition of the overlying fossiliferous clastic deposits. Such a contact does not occur in the upper cave, where a completely sharp contact occurs between pure speleothems and the clastic deposits. Here a long hiatus in deposition is indicated.

*Clastic phases I and II*

An 8-m stratigraphic section of clastic deposits, laid down over PIIS, is evidence for retreat of the cliff face and an opening to the surface. The sharp contact between pure PIIS and clastic sediments, together with the lack of clastics incorporated in the PIIS, suggests that a hiatus may have occurred after PIIS.

The clastic material consists of two distinct phases, clastic phase I (CPI) and clastic phase II (CPII). The initial phase (clastic phase I, or CPI) is represented by a relatively small amount of material. CPI consists of two distinct facies. Facies A consists of sterile fine-grained red silt representing flood wash. Facies B consists of a layer of coarse semi-angular to subrounded conglomerate and breccia representing periods between major flooding where slope and flood debris is calcified together. In the upper cave, large angular clasts (3–8 cm) of material were deposited in a small channel within the undulating flowstone floor and were calcified to form a coarse, purple, talus slope breccia. The purple color suggests the presence of collophane and thus the presence of a bat roost. Fossils in the deposits include bovid teeth and are heavily fractured and indurated by a carbonate cement matrix. This suggests material that has been washed in from the surface. This deposit is then overlain by the interstratified layers of facies A and B alternating on a scale of about 15–20 cm. In the lower cave, a direct change from PIIS to the fine-grained red cave silt of clastic phase II (CPII) is observed. The coarser layers present in the upper cave are not represented in the lower cave, which suggests that it lay beyond reach of the talus slope.

The clastic phases (I to III) of the sequence are all dominated by calcified red silts containing rounded cobbles up to 20 cm diameter. At the rear of the ancient cave, there was no talus slope; instead a flat mud floor occurs that possibly represents the winnowing of fines from the entrance talus of CPII, which has long since been eroded away. Whereas part of this entrance talus may have been derived from a colluvial origin via collapse of the cave entrance, the majority of sediments appear to be of alluvial origin, unlike at many of the other sites (Herries, 2003).

From a taphonomic point of view, the cavity became relatively flat floored, and a large accumulation of fossil bones indicates that it operated as a den. Similarly, in the upper cave, there are blackened, magnesium dioxide-stained bones densely scattered throughout a series of red silt layers. The density of the bone accumulations, containing the relatively complete bones of large-sized bovids in association with both hyena coprolites and skeletal remains, suggests that this area functioned as a hyena den (the UCD). There is some evidence of secondary redistribution of the UCD fossil material in a scattering of similar, but smaller, blackened fossil material that can be seen in the section running from the UCD to the lower cave.

The mud floor deposit of CPII has a total thickness of approximately 8 m and extends approximately 2 m above the bone deposit. At the top of the CPII, there are local speleothem layers and desiccation cracks in mud. Rounded pebbles are also present suggesting that cyclic periods of flooding occurred. The densest area of in situ bone material occurs at the end of CPII on the eastern side, directly above the upper cave and stratigraphically higher than the UCD. A large block of this material, the Crowbar Block, was removed for safety reasons in 2002 and its faunal remains are currently being prepared. A preliminary observation of surface fossils indicate that it has a similar faunal assemblage to that of the lower UCD fossil material, consisting primarily of large bovids. Currently, the exact stratigraphic relationship of this block to other deposits is problematic due to the obscuring effect of the overlying tufa as mentioned earlier.

### *Phase III speleothem (PIIIS)*

The CPII deposits are overlain by the phase III speleothem (PIIIS). This represents a phase of major speleothem deposition that interleaves locally with red silt layers that are still being deposited on the north east side of the site. PIIIS consists mainly of flowstones covered by massive, coralloid speleothem. This area has been, and continues to be, a major seepage water route. There are extensive tufa deposits, extending from 25 m up the cliff face, parts of which appear to have been inactive for some time. Dating of the phases of the tufa and travertine is currently underway. The tufa and travertine layers that are formed in the open air may be distinguished from the older compact subterranean speleothem by their porous and more friable nature where rotted moss, ferns and other vegetation have left root holes in the structure. The PIIIS layer is exposed on ‘the ledge’ and easily identified by a large (1 m) coralloid covered stalagmite.

### *Clastic phase III (CPIII)*

PIIIS is overlain by a series of calcite-rich, fossiliferous, grey silts and red cave silts with cobbles, termed clastic phase III (CPIII). CPIII may have originally been deposited for another 5–10 m above its current level, based on small, inaccessible remnants that can be seen adhering to the cliff face. Only the base of CPIII was sampled during this study and the fossil material from this deposit has not yet been completely sampled.

## Paleomagnetism

Within the main northern area, in situ block samples were collected from all recognized units whose stratigraphic positions were determined to be secure. In some areas, single rope technique (SRT; Herries et al., 2001) was used to obtain otherwise inaccessible samples. Samples were oriented in situ using a Suunto clinometer and magnetic compass; the azimuths were corrected for local declination. No magnetic distortion was seen due to overlying deposits.

The blocks were subsequently drilled in a zero field cage back at the Liverpool University Geomagnetism Laboratory. This was in order to prevent the acquisition of a rotational remanent magnetization (RRM) that has been noted as a problem at Sterkfontein and the Makapansgat Limeworks (Herries, 2003) and is caused by the highly viscous nature of the samples. For each sample, two 20-mm diameter cores were drilled and subsequently cut into a series of 25 × 20 mm subsamples to create an average of 2 to 4 subsamples from each block. The outer 10 mm of the cores were discarded so as to remove any weathered surfaces and any possible effects from the mine blasting. Sampling was undertaken away from miners’ shot holes to avoid any potential resetting of the magnetic signal by shock-induced remanent magnetization, as potentially identified at Sterkfontein (Herries, 2003). Drilling was undertaken at right angles to the layering of the silts and speleothems so as to obtain maximum resolution in deposition and hence of time. The more easily magnetizable grains may lose or acquire a remanence in later fields and any resulting magnetization is known as a viscous remanent magnetization (VRM). Usually, the VRM has a direction different to the primary magnetization and so has to be minimized in transport and storage and magnetically cleaned in the laboratory. Samples were thus stored after drilling and before measurement in a zero field cage and any remaining hard VRM was removed during measurement by standard cleaning techniques.

The sum of all sample magnetizations constitutes its natural remanent magnetization (NRM). Sample NRMs were measured using a FIT cryogenic SQUID-based spinner magnetometer with a minimum sensitivity of $0.2 \times 10^{-8}$ Am$^2$ kg$^{-1}$. Sample NRMs ranged from $150 \times 10^{-8}$ Am$^2$/kg in the cave silt samples to below $0.2 \times 10^{-8}$ Am$^2$/kg in the speleothem samples, which is relatively low for South African cave deposits (Herries, 2003). Consequently, NRMs could only be measured for approximately 10% of the speleothem samples from the PIIS. Due to the friable and calcified nature of most of the deposits, alternating field demagnetization (AFd) was initially used to magnetically clean the NRMs in order to isolate the samples characteristic remanent magnetization (ChRM). However, many of the sediment samples showed low magnetic stability at fields above 20–40 mT. Consequently, a hybrid strategy involving initial magnetic cleaning of VRM using 5 mT stepwise alternating field demagnetization, followed by 50°C stepwise thermal demagnetization, was employed. This hybrid approach was designed to isolate a primary remanence at lower temperatures before any potential mineral alteration and calcite expansion occurred. The field required to remove the VRM was generally around 10–15 mT. The cleaned characteristic remanence (ChRM) was in most cases relatively stable up to temperatures of between 550° and 600°C and indicated magnetite as the main remanence carrier. This ChRM was then taken to be the sample’s primary remanence, that is, the post-depositional remanent magnetization (pDRM) acquired at or near the time of deposition. Pure speleothem samples showed good stability to AFd at fields up to 140 mT and little evidence of VRM. However, many samples from the PIIS gave relatively scattered directions due to lack of clastic inclusions and resultant low magnetic intensity. Comparative sister samples were also thermally demagnetized in 50°C increments to a temperature of 700°C.

After magnetic cleaning, remanence directions of subsamples were determined using principal component analysis of orthogonal vector and stereoplots (Kirschvink, 1980). Fisher (1953) mean directions were then calculated for each block sample (Table 1). The polarities were assigned according to whether their directions were within a 40° cone of the normal or reversed field, that is, 0° to −40° were assigned to a normal field and 140° to 220° were assigned to a reversed field. The best results as measured by low angular dispersion about the mean cleaned directions came from flowstone samples taken from the PIIIS (BCPU03–05; Fig. 5b) and from a series of calcified silt samples from CPII (BCP13–14) that were subjected to the hybrid demagnetization method.

The primary remanent magnetization of sediments and speleothem is acquired when magnetic oxide grains settle in still water and are aligned in the direction of the Earth's ambient magnetic field (Latham and Ford, 1993). This is referred to as a depositional remanent magnetization (DRM). In sediments, post-depositional compaction upon dewatering causes a slight realignment of the magnetic grains to produce a post-depositional remanent magnetization (pDRM). As dewatering of the silts in Buffalo Cave is thought to follow each flood event, any pDRM is likely to have formed with only a short time lag after deposition. Therefore any pDRMs would be unlikely to have any significant effect on the recorded polarity. The magnetizations of most stalagmites and flowstones appear to arise either from the detritus of flood deposition or from some kind of chemical interaction with iron bound in organic materials.

Samples taken from more brecciated layers in the CPI of the upper cave gave highly scattered directions that are probably due to the dominance of some magnetically strong clasts that are oriented in directions other than the ambient Earth's field. Some samples from layers showing mud cracks yielded inclinations that were shallow when compared to the average inclination expected for this latitude. The inclination at Makapansgat for an axial dipole is −41°, whereas such samples showed inclinations of −20 to −30°. It is well known that clastic deposits can show shallow inclinations of several degrees due to particle settling, slope effects and compaction (see, e.g., Verosub, 1977; Brennan, 1993). The majority of calcified silts from CPII on the other hand are subhorizontally bedded and do not appear to have suffered major bedding errors from slope processes. Despite these effects, it is considered that the magnetizations could be safely assignable to one polarity or the other, although the defining of more intermediate polarities as one might expect in a polarity transition must be made with caution.

Table 1
Fisher mean directions, mineral magnetic parameters and polarity determined for each of the individual sample blocks throughout the Buffalo paleocave sequence

| Sample | Sample stratigraphic unit | Location | Declination (°) | Inclination (°) | No. samples | $\alpha_{95}$ or MAD | Polarity | $\kappa_{LF}$ (10–5) | $\chi_{FD}$% | $T_C$ (°C) | $H_{cr}$ (mT) | RS |
|---|---|---|---|---|---|---|---|---|---|---|---|---|
| BCPU01 | CPIII | L | 183.3 | 47.8 | 4 (1) | 26.9 | R | 33.33 | 9 | 575 | 25 | 0.61 |
| BCPU06 | PIIIS | L | 195.2 | 34.7 | 2 (0) | 78.5 | R | 289.67 | 14.79 | 576 | 27 | 0.54 |
| BCPU05 | PIIIS | L | 190.7 | 40.2 | 2 (0) | 10.9 | R | 69.84 | 11.22 | 564 | 25 | 0.67 |
| BCPU04 | PIIIS | L | 194.5 | 28.1 | 2 (0) | 8 | R | 75.84 | 7.91 | 578 | 27 | 0.52 |
| BCPU03 | PIIS | L | 198.7 | 28.4 | 2 (0) | 44.6 | R | 49.17 | 15.93 | 585 | 26 | 0.52 |
| BCPU02 | CPII | L | 199.5 | 26.6 | 2 (0) | 51.7 | R | 280 | 10.83 | 574 | 25 | 0.53 |
| BCPL14 | CPII | UC | 174.5 | 52.4 | 2 (0) | 6.5 | R | 204.5 | 12.71 | 589 | 26 | 0.58 |
| BCPL13 | CPII | UC | 166.2 | 27.9 | 4 (0) | 15.6 | R | 277.17 | 11.73 | 590 | 25 | 0.57 |
| BCPL12 | CPII | LC | 199.6 | 33.5 | 2 (0) | 15.5 | R | 295.83 | 13.75 | 570 | 25 | 0.57 |
| BCPP11 | CPII | LC | 102.1 | 29.9 | 2 (0) | 22.3 | I | 250 | 11.58 | 578 | 25 | 0.52 |
| BCPL10 | CPII | LC | 266.7 | 47 | 2 (0) | 14.8 | IR | 228.5 | 13.64 | 580 | 25 | 0.6 |
| BCP06 | CPII | UC | 152 | 13.8 | 2 (0) | 16 | IR | x | x | x | x | x |
| BCP05 | CPI | UC | 153.7 | −63 | 3 (0) | 4.6 | I | 54.7 | 10.79 | 568 | 27 | 0.66 |
| BCP04 | CPI | UC | 46.9 | −31.1 | 1 | 19.1 | IN | 180 | 11.22 | x | x | x |
| BCP03 | CPI | UC | 45 | −39.3 | 1 | 21.2 | IN | 50 | 8.6 | x | x | x |
| BCP02 | CPI | UC | 312.9 | −42 | 1 | 2.8 | IN | x | x | x | x | x |
| BCP15 | CPI | UC | 357.2 | −48.4 | 2 (0) | 73.1 | N | 8.17 | 6.12 | 595 | 27 | 0.56 |
| BCP18 | PIIS | UC | 347.4 | −46.3 | 2 (0) | 23.8 | N | x | x | x | x | x |
| MCP16 G | PIIS | LC | 291.3 | 1.6 | 2 (0) | 18.7 | I | 9.34 | 7.92 | 587 | 25 | 0.60 |
| MCP16 | PIIS | LC | 195.6 | 47.3 | 4 (0) | 36.9 | R | x | x | x | x | x |
| BCP01 | PIIS | LC | 192.8 | 35.5 | 4 (3) | 15.6 | R | x | x | x | x | x |
| BCP25a | PIIS | LC | 37.2 | −26.7 | 1 | x | N | x | x | x | x | x |
| BCP25b | PIIS | LC | 31.3 | −13.9 | 1 (2) | x | IN | x | x | x | x | x |
| BCP17 | PIIS | LC | 97.2 | −40.2 | 4 (2) | 13.1 | I | x | x | x | x | x |
| | | | | | | | mean | 147.25 | 11.11 | 579 | 26 | 0.57 |

Polarity: IR = intermediate reversed; IN = intermediate normal, I = intermediate. $\alpha_{95}$ = confidence parameter at 2 standard deviations. $\kappa_{LF}$ = non-mass-specific low-frequency magnetic susceptibility. $\chi_{FD}$% = frequency dependence of magnetic susceptibility; $T_C$ = Curie temperature; $H_{cr}$ = coercivity of remanence; RS = low-temperature magnetic susceptibility ratios (−196°/+25°C). Mineral magnetic measurements represent measurements from single sister specimens from each paleomagnetic block sample, except for $\kappa_{LF}$ and $\chi_{FD}$%, which are means for all subsamples. Number of samples: number in brackets represents the number of samples rejected.

## Mineral magnetism

A suite of standard mineral magnetic (rock magnetic) tests were carried out to determine the magnetic mineralogy and characteristic grain sizes of the various deposits and these are summarized in Table 1. Magnetic susceptibility ($\chi$) measurements were undertaken using the Bartington MS2B magnetic susceptibility and low-temperature magnetic susceptibility ($\chi_{LT}$) system for frequency dependency and low temperature measurements. Most samples have a very high percentage (9–13%) of frequency-dependent values of magnetic susceptibility ($\chi_{FD}$%; mean values for block samples given in Fig. 4a), which indicates that they have a high proportion of fine to ultrafine grain sizes near the superparamagnetic to single-domain boundary. $\chi_{FD}$% and $\chi_{LF}$ (low frequency magnetic susceptibility) show some correlation and fall into two distinct groups (mean values for block samples are given in Table 1). This accounts for the high viscosity of the samples and strong-overprinting hard VRM component that is noted during magnetic cleaning. The cause for such unusually high values is thought to relate to the age of the South African landscape, the long-term weathering and continuous burning of sediments by natural bushfires. Low-temperature magnetic susceptibility (Fig. 4b) curves also confirm a significant fraction of superparamagnetic grains (Table 1). Thermomagnetic curves (Fig. 4c), hysteresis loops and isothermal remanent magnetization (IRM; Fig. 4d) acquisition curves and backfields were undertaken on a magnetic measurements variable field translation balance (VFTB). Thermomagnetic curves gave Curie points ($T_C$) with a mean of 579°C indicating that the main remanence-carrying mineral is magnetite for most samples (Fig. 4a). Some higher $T_C$ and lowering in magnetization after heating to 700°C indicate the probable presence of thermally stable maghemite. IRM acquisition curves (Fig. 4d) show that the samples are dominated by a low-coercivity ferromagnetic mineral. The sample does not saturate until close to 300 mT, suggesting that these ferromagnetic minerals are in the single-domain grain size region. A small proportion of pigmentry hematite is also indicated by nonsaturation of remanence in higher fields. It is this mineral that gives the sediment its bright red coloration. IRM unmixing curves show the presence of 3 distinct populations representing low, medium and high

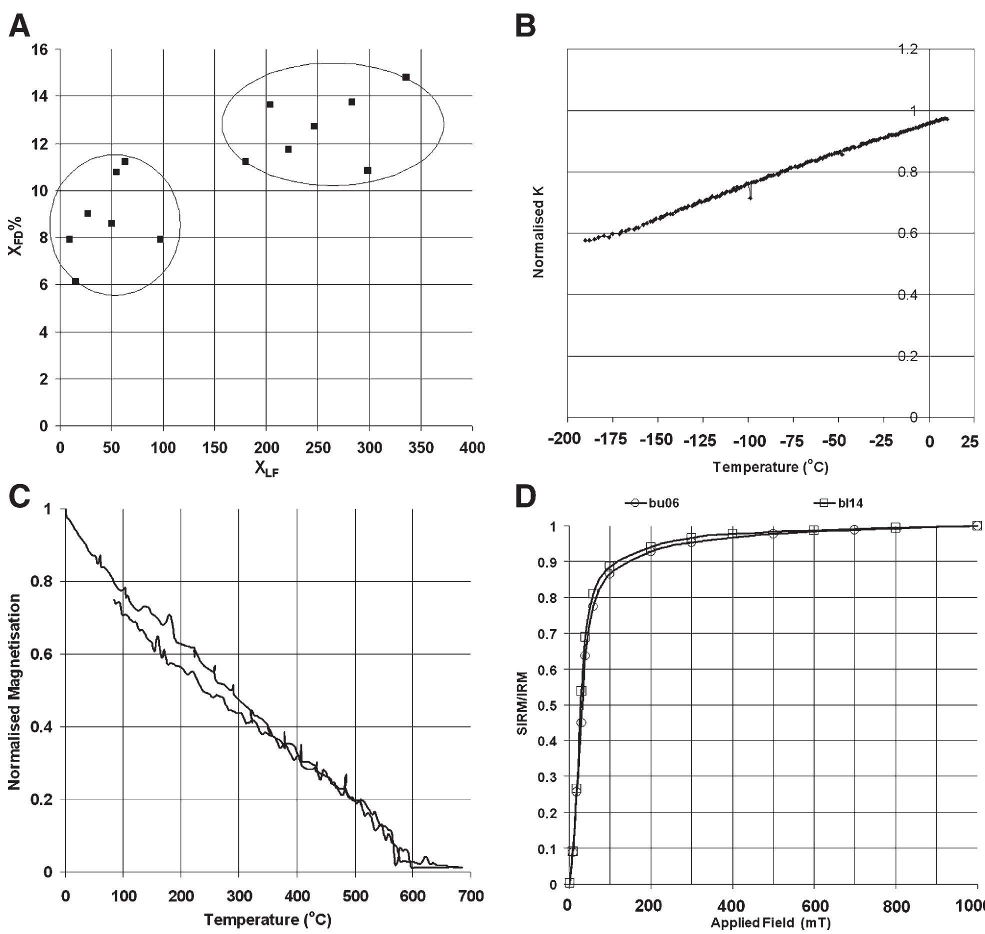


Figure 4. (A) Log low-frequency magnetic susceptibility ($\chi_{LF}$) versus percentage frequency dependence of magnetic susceptibility ($\chi_{FD}$%). (B) Low-temperature magnetic susceptibility ($\chi_{LT}$) for Buffalo Cave paleomagnetic block samples showing that the samples are dominated by ferromagnetic minerals with grain sizes across the superparamagnetic to single domain boundary. (C) Thermomagnetic curve with a Curie point of 580°C, indicating that the samples are dominated by magnetite. (D) Isothermal Remanent Magnetization acquisition curves for two silts samples from Buffalo Cave showing the dominance of a single-domain ferromagnetic mineral (magnetite), with a small proportion of anti-ferromagnetic material (hematite).

coercivity minerals, which relate to superparamagnetic/single-domain boundary magnetite, stable-single-domain magnetite, and ultra-fine-grained pigmentary hematite in decreasing proportions.

## Biochronology

Excavations for faunal remains focused on the collapsed deposits in the floor of the upper cave. For this paper, only bovid specimens from these recent excavations were used in the biochronology analyses. These species were all recovered in the late 1990s with most of the processing and identifications done in 1999. The specimens are thus derived only from the CPI and CPII deposits and are not the same as the faunal list published by Kuykendall et al. (1995), many of which came from ex situ breccia blocks with unknown provenance.

Unless otherwise stated, currently accepted first (FAD) and last (LAD) appearance data of these bovids (Vrba, 1995) were used to infer the most likely depositional time period by using the overlap of the dates of different species (Table 2). If new dates have been obtained for the deposit then these were preferentially used. Because the absolute dating of South African cave deposits is problematic, we noted if FADs or LADs of species are known *only* from southern Africa. Almost all of the bovids are known from east Africa. All of the radiometrically dated east African bovids represented in this Buffalo Cave fauna essentially overlap in the interval from 960,000 yr to 600,000 yr. There is a distinct taphonomic bias evident at Buffalo Cave towards a preponderance of large alcelaphine bovids.

Identifications of horn cores and teeth of these species were compared to descriptions and material from eastern Africa. The only taxon previously unknown in South Africa is *Parmularius rugosus*, which occurs in Olduvai Bed II (FAD) between 1.76 and 1.56 Ma, and Olduvai beds IV HWK (LAD) between 780,000 and 700,000 yr. As earlier *Parmularius* taxa are present in South Africa at Makapansgat Member 3 (3.04–2.58 Ma; Herries, 2003), it is possible that this is a unique species, but specimens appear to represent *P. rugosus*.

The genus *Pelorovis* first appears at between 3.36 and 2.68 Ma in the Tula Bor Formation at East Turkana (Behrensmeyer et al., 1997) and at 2.38 Ma in Shungura C8 (Vrba, 1995). It is perhaps also present in Swartkrans Member 2 dated to somewhere between 1.6 and 1.1 Ma based on varied age estimates and methods (De Ruiter, 2003). However, significant mixing and reworking of fossils is suggested in Member 2 of Swartkrans by Curnoe et al. (2001). Moreover, the fossils are tentatively assigned to the *Pelorovis* sp. (*antiquus*), which first occurs in Olduvai bed IV GC between 780,000 and 600,000 yr (FAD) in east Africa and at Cornelia-Uitzoek in South Africa between 1.0 Ma and 800,000 yr (FAD; James Brink, personal communication, October 2005) and at Nelson Bay Cave in South Africa between 12,000 and 9000 yr (LAD). *Pelerovis* also occurs at Gladysvale in sediments dated to between 780,000 and 578,000 yr by ESR and paleomagnetism (Lacruz et al., 2002).

*Hippotragus gigas* has an FAD of around 2.5 Ma in east Africa. In South Africa, it appears at Elandsfontein, considered to be roughly 700–600,000 yr (James Brink, personal communication, October 2005). Hippotragine teeth have also been recovered from the oldest layers at Florisbad, dated to

Table 2
Main FAD and LAD data from Vrba 1995 unless otherwise stated

| Species | FAD (Ma) | LAD (Ma) | East African sites | South African sites |
|---|---|---|---|---|
| *R. arambourgi* | 1.79 [a] | 0.60 [b] | Olduvai III (also recovered) | Swartkrans M1 (FAD); Elandsfontein (LAD) |
| *P.* cf. *rugosus* | (1.76) | (0.7) | Olduvai II (FAD); Olduvai IV HWK (LAD) | No other localities |
| *M. kattwinkeli* | (2.80 [b]) 2.56 [c] | (0.6) | Chiwondo (FAD); Olduvai IV GC (LAD) | Sterkfontein 4 (FAD) |
| *Antidorcas* cf. *recki* | (3.36 [d]) 2.56 [c] (2.38) | 0.60 [b] | Tulu Bor (FAD) Shungura F3 (FAD) | Elandsfontein (LAD) Sterkfontein 4 (FAD) |
| *H. gigas* | (2.57) | 0.60 [b, e] | Shungura C8 and Gamedah, middle Awash (FADs) | Elandsfontein (LAD) |
| *Pelorovis* sp. *(antiquus)* | (0.78) 1.0–0.8 [b,e] | 0.009 | Olduvai IV (FAD) | Nelson Bay Cave (LAD); Cornelia-Uitzoek (FAD) |
| *Taurotragus* cf. *oryx* (lineage dates) | (0.96) 1.95 [c, f] | Extant | Olduvai IV (FAD) | Gondolin (FAD) |
| *R. arundinum* | 1.79 [a] | Extant | | Swatkrans M1 Hanging; Remnant (FAD) |

[a] Dates from Curnoe et al. (2001). The date is given as a maximum error value for upper or lower age limits of the deposit.
[b] For taxa without paleomagnetic or radiometric FAD or LAD, we give the site and the site date with an approximate date for the species FAD or LAD based on biostratigraphy. Dates in parenthesis (-) are from east Africa and all others are South African.
[c] Dates from Herries (2003).
[d] Dates from Behrensmeyer et al. (1997).
[e] Dates from Brink (2002; personal communication, October 2005).
[f] Dates from Adams and Conroy (2005).

between 326,000 and 115,000 yr (LAD) by ESR (Grun et al., 1996), but a species has not been positively identified (James Brink, personal communication. October 2005). *Antidorcas recki* is found in east African in the Tulu Bor Formation (FAD; Behrensmeyer et al., 1997) between 3.36 and 2.68 Ma and at Omo in Shungura F3 between 2.38 and 2.28 Ma (FAD; Vrba, 1995). In South Africa *A. recki* and *Megalotragus kattwinkeli* are both found in Sterkfontein Member 4, which has been dated to between 2.58 and 2.14 Ma (South African FAD) using paleomagnetism (Herries, 2003) and provides South African FADs for both. *M. kattwinkeli* is also found in Malawi dated by biochronology to between 2.8 and 2.5 Ma (FAD) and in east Africa the species appears at Olduvai Gorge bed IV GC between 780,000 and 600,000 yr (LAD). *A. recki* is found at Elandsfontein in South Africa at a similar time period of around 600,000 yr (LAD).

Although the extant *Redunca arundinum* is solely a southern African taxon reported from Elandsfontein at around 600,000 yr, it tentatively also falls in this age bracket as De Ruiter (2003) reports the potential occurrence of this taxon from the Member 1 Hanging Remnant of Swartkrans (FAD) dated by ESR to 1.63 ± 0.16 Ma (Curnoe et al., 2001). This is the only identification of this species at such an early date. *Rabaticeras arambourgi* also occurs at both these sites with Elandsfontein providing Member 1 the LAD and Swartkrans Member 1 the FAD. This species also occurs at Gladysvale between 780 and 578,000 yr (Lacruz et al., 2002) and provides a potentially more secure LAD.

The extant Taurotragus cf. oryx occurs in Olduvai bed IV LK-RK, which is dated between 960,000 and 600,000 yr (FAD). In South Africa, it occurs at Plovers Lake at around 1.0 Ma based on biostratigraphy (Thackeray and Watson, 1994) and at Gondolin between 1.95 and 1.78 Ma (Herries, 2003; Adams and Conroy, 2005; Herries et al., in press). Based solely on biochronology, the optimal dates for the depositional unit discussed here is thus between 960,000 and 600,000 yr based on correlation with east African sites and between 1.0 Ma and 600,000 yr based on correlation with South African sites.

## Magnetobiostratigraphic chronology

The geomagnetic polarity time scale (GPTS) (see Ogg and Smith, 2004) consists of a series of magnetic chrons of either normal or reversed polarity and, within them, shorter events of opposite polarity. The reversals of the GPTS do not occur regularly, and reversal intervals are not of the same length, thus making sections of the GPTS sufficiently distinctive for use as a chronology for a target sequence of sediments. The ideal requirements for magnetostratigraphic dating of a depositional sequence are that (1) samples from the deposits possess a primary remanent magnetization of sufficient strength that, after the removal of any soft (viscous) components, they are measurable in a magnetometer; (2) the deposits were laid down at about the same depositional rate throughout the sequence, with no hiatuses, so that reversal zones are not distorted or omitted; and (3) the sequence has a sufficient number of reversals that its record can be identified uniquely with a part of the dated GPTS.

The magnetostratigraphy at Buffalo Cave consists of a reversed polarity for much of the PIIS, although two samples from a basal block sample (BCP17; Fig. 5l) have an intermediate direction of magnetization and two other subsamples from a second block (BCP25; Fig. 5l) show an intermediate normal direction and a normal direction of magnetization. This may suggest deposition at a polarity transition, perhaps the beginning or end of the Olduvai normal polarity event at between 1.95 and 1.78 Ma. Above these basal samples, the next 2.3 m of PIIS flowstone was magnetically too weak to provide polarity data. At present, the only indication as to the length of time represented by the flowstone comes from its marked oxygen and carbon stable isotope periodicity, in which the number of Milankovitch cycles indicates that it grew over several hundred thousand years (Hopley, 2004). The top of the flowstone shows predominantly reversed directions of magnetization (BCP01, Fig. 5k; BCP16, Fig. 5j). Intermediate (BCP16; Fig. 5i) directions of polarity are noted for the collophane crust that occurs at the contact between the PIIS and the overlying CPII deposits in the lower cave. This perhaps indicates a change from a reversal to a normal polarity. Normal directions are also noted for a block from the very top of the flowstone sequence in the upper cave (BCP18; Fig. 5h). This may relate either to the beginning of the normal polarity period noted in CPI or may actually be related to lower in the flowstone sequence and the Olduvai event between 1.95 and 1.78 Ma. No stratigraphic link can be made between the flowstone in the upper and lower cave as can be accomplished for the clastic deposits.

Despite this interpretive problem, the presence of intermediate directions of magnetization in the top section of the lower cave flowstone (PIIS) suggests that the flowstone may have been deposited towards the end of a period of reversed polarity. The CPI silts record normal then intermediate normal (BCP2–4; Fig. 5f–h) polarities and are then followed by intermediate directions (BCP05, Fig. 5e; BCP06, Fig. 5d). A hiatus may be present between the deposition of PIIS and CPI, so the normal polarity period is not represented entirely. The samples from CPII (Fig. 5c), PIIIS (Fig. 5b) and CPIII (BCPU06; Fig. 5a) all lie in a period of reversed polarity, the end of which is not reached by the top of the remaining section.

The difficulties inherent in the recovery of magnetostratigraphic dating of cave sediments have been well outlined by Bosák et al. (2003) and Buffalo Cave shows them, as it only fulfils the first of the three ideal criteria outlined above. Given the lack of precise dating of fossil localities in South Africa and because of the possibility that southern Africa may have functioned as a separate faunal province from east Africa, ideally the polarity analyses should be made independent of considerations from faunal (biostratigraphic) analysis. At Buffalo Cave, the sequence has not yielded sufficient reversals to fit it to the GPTS without assistance from faunal dating and the sequence includes alternating layers of speleothem and clastic sediments that will have been laid down at vastly different rates. Clastic sediments

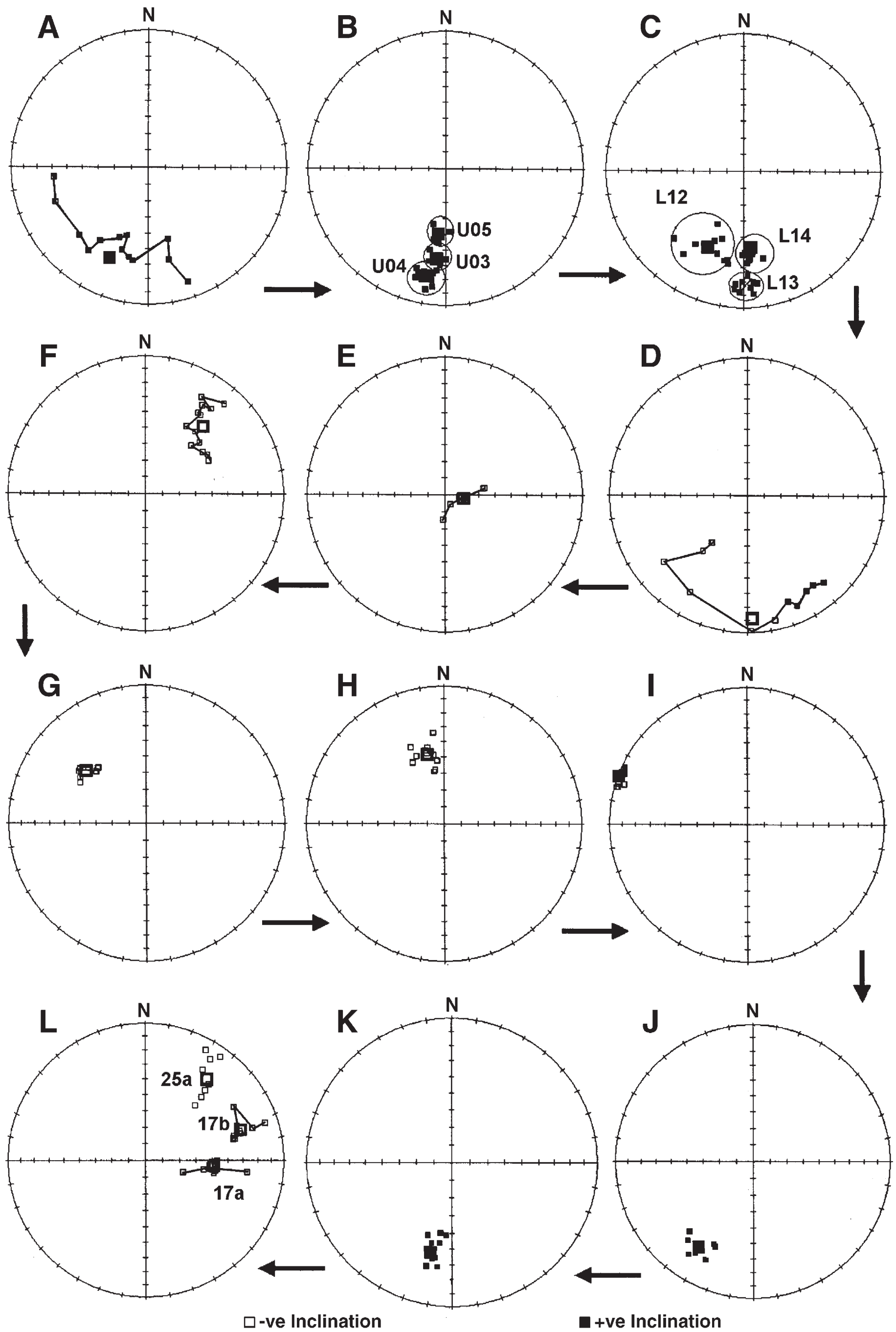


Figure 5. Circular (stereo) plots showing the polarity transitions from uppermost CPIII to basal PIIS. (A) Reversed sample BCPU06 from CPIII; (B) reversed samples BCPU04–05 from SPIII; (C) reversed samples BCP12–14 from CPII; (D) reversed intermediate sample BCP06 from CPII; (E) intermediate–intermediate sample BCP05 from CP1; (F) normal sample BCP04 from CP1; (G) normal intermediate sample BCP03 from CP1; (H) normal sample BCP18 from PIIS; (I) intermediate sample BCP16G from the guano layer of the PIIS; (J) reversed sample BCP16 from PIIS; (K) reversed sample BCP01 from PIIS; (L) intermediate samples BCP17 and intermediate-normal sample BCP25 from the base of PIIS.

were deposited over thousands of years, whereas speleothems are deposited over hundreds of thousands of years. This is compounded by the existence of a possible hiatus between the end of the basal speleothem deposition of PIIS and the deposition of the bulk of clastic sediments beginning with CP1 and an uneven deposition of the various phases in different parts of the paleocavern. However, careful stratigraphic mapping has aided in the reconstruction of a detailed and relatively unbroken stratigraphic sequence for the western deposits. It is believed that the faunal representations are sufficiently well constrained by east and South African FAD and LAD dates that the associated magnetostratigraphic section can be matched fairly confidently to the GPTS by taking into account relative depositional rates, and the presumed stretch and compression of certain sections of the stratigraphy.

Establishment of the site chronology is then dependent on identification of the age of one normal subchron within a predominantly reversed section (Fig. 6). First, the polarity changes cannot be fitted to anywhere within the Brunhes Chron (780,000 yr to present) because the two periods of reversal are too long to match any known reversal events within this period and the sequence ends with a section of reversed polarity. As such the site must be older than the last magnetic reversal, the Bruhnes–Matuyama boundary at 780,000 yr. This is in partial contradiction with the identification of the species *Pelorovis* sp. (*antiquus*), which has only been found in deposits younger than 780,000 yr in east Africa. If this specimen is indeed *Pelorovis* sp. *antiquus* then it would push the FAD of this species back to between 1.07 Ma and 780,000 yr, rather than between 780,000 and 600,000 yr as it currently stands. Both *P.* cf. *rugosus* and *M. kattwinkeli* are unlikely to be represented in any deposits after 600,000 to 700,000 yr.

At the earliest, the Olduvai normal event within the Matuyama reversed chron at between 1.95 and 1.78 Ma could accommodate some, but not all, of the faunal data. The Olduvai event is also suggested to occur earlier in the PIIS sequence. Another potential period of deposition of this normal polarity period would be the Cobb Mountain event at between 1.19 and 1.17 Ma (Ogg and Smith, 2004). This would date the fossil bearing part of the site to between 1.19 and 1.07 Ma. However, the most likely period that accommodates the section of normal

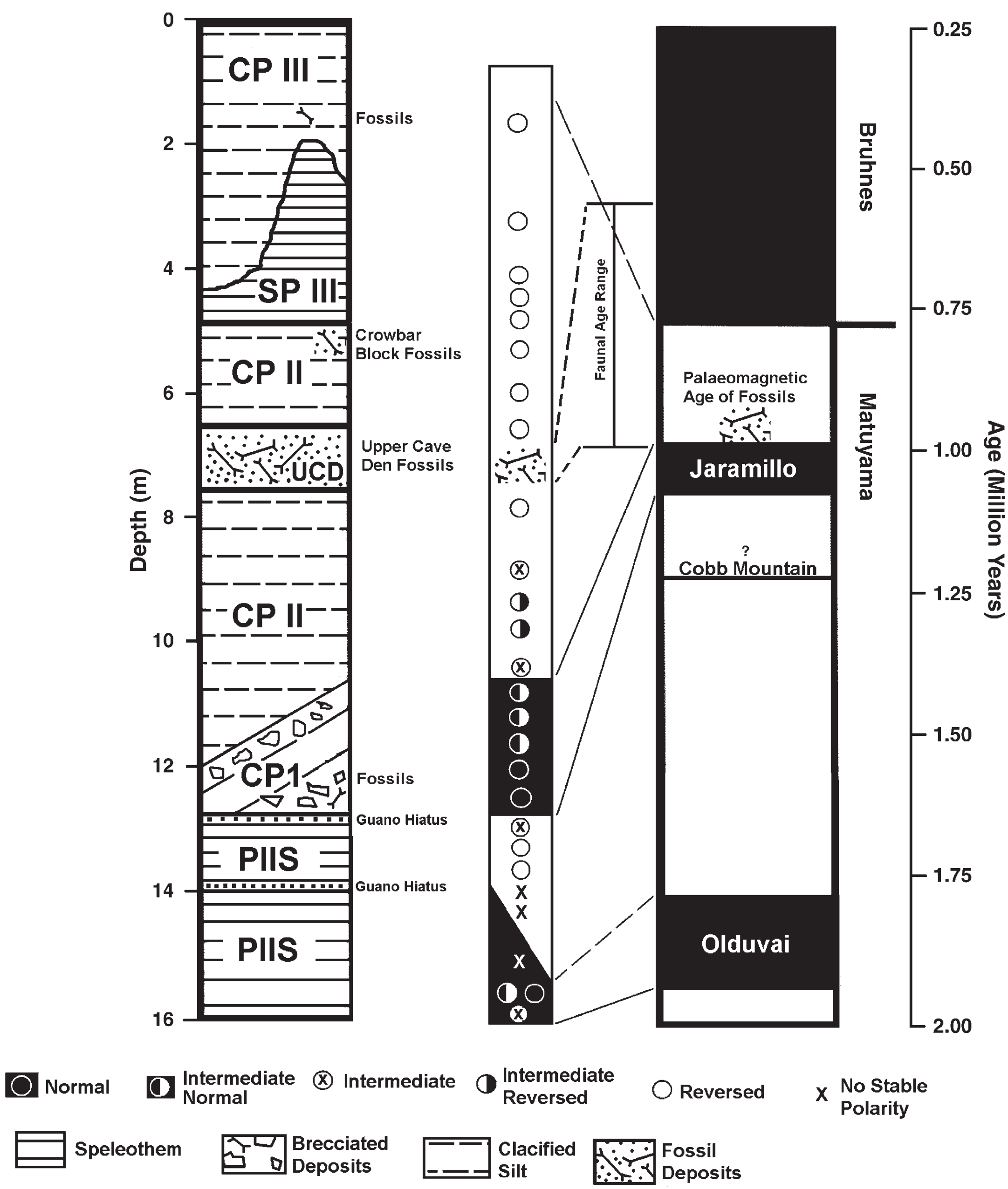


Figure 6. Stratigraphy, polarity data and magnetostratigraphy of the Buffalo Cave fossil deposits compared to the geomagnetic polarity time scale for the last 2 million years.

polarity and all the faunal data is the Jaramillo normal event at between 1.07 Ma and 990,000 yr.

Based on this polarity interpretation at the site and faunal age ranges, the PIIS appears to date to between 1.95 Ma and some time after 1.07 Ma. This fits well with estimates of its duration and pattern from isotopic data, which suggests that the normal event potentially seen in the base of the PIIS is the Olduvai (Hopley, 2004). CPI dates to the Jaramillo between 1.07 Ma and 990,000 yr, although the intermediate directions that dominate this deposit suggest it was deposited closer to 990,000 yr. CPII, PIIIS and CPIII deposits all show a reversed polarity and thus date to the Matuyama reversed chron between 990,000 and 780,000 yr. The main faunal layers are within CPII, which is composed of fairly rapidly deposited silts laid down soon after the end of the Jaramillo normal event at 990,000 yr. Some fossils are noted in CPIII but none have as yet been sampled. These fossils are likely to date towards the end of the Bruhnes reversed chron at 780,000 yr, as the underlying PIIIS consists of relatively slow forming speleothem that is the dominant depositional regime during the identified reversed period. Similarly, CPII fossils are likely to date closer to 990,000 yr than 780,000 yr. In total, the deposits cover the period between approximately 1.95 Ma and 780,000 yr, but the main faunal-bearing sediments (CP1 and CPII) are deposited close to 990,000 yr with a total range for the faunal-bearing deposits between 1.07 Ma and 780,000 yr. Figure 6 shows the magnetic polarities set against the major stratigraphic units with the preferred match to the GPTS.

## Discussion

Buffalo Cave provides a window into faunal succession for a relatively underrepresented period (the late early Pleistocene) in the paleontological record of southern Africa and is an important site for the paleoenvironmental information it provides for this geographic and temporal context. The fossil-bearing portion of the site is dated to between 1.07 Ma and 780,000 yr, a period intermediate in age between the mainly Pliocene Makapansgat Limeworks paleocave at 4.18 to 2.16 Ma (Herries, 2003) and the middle Pleistocene Cave of Hearths/Historic Cave sequence at less than 780,000 yr. It is of great interest that these sites lie within a couple of miles of each other on the Makapansgat Farm and, taken together with other smaller localities (Grand Canyon Rockshelter, Historic Cave, Hyena Cave and Horse Mandible Cave), present an intermittent fossil-bearing sequence of deposits from 4.18 Ma up to historic times. Only a few other South African fossil localities exist for the late early to middle Pleistocene transition and cover the same time period as Buffalo Cave. These include the Gladysvale external deposits (GVED), which are dated to between approximately 780,000 and 576,000 yr (Lacruz et al., 2002; Herries, 2003); Plovers Lake, which is dated to around 1.0 Ma (Thackeray and Watson, 1994); and Cornelia-Uitzoek, dated to between roughly 1.0 Ma and approximately 800,000 yr (Brink, 2002).

The majority of the Buffalo Cave fauna, here estimated to be dated to soon after 990,000 yr, corresponds to a major cooling trend in Southern Africa centered on 900,000 yr (Klein, 1977) that is possibly an influential factor in the extinction of the *Paranthropus* species. In east Africa some of the last specimens of *Paranthropus*/*Australopithecus boisei* were found at Chesowanja dating to just over 1.0 Ma (Wood, 1999). At present, only the single hominin tooth of a species of Homo from Cornelia-Uitzoek (Brink, 2002) has been recovered from deposits dated to this period in South Africa. It remains to be seen whether this absence of evidence is also evidence of absence of at least the robust hominine lineage. Preliminary analysis of pollen from cave silts (Schoenwetter, 2000) suggests that a very different climate existed in the Makapansgat region during the depositional period represented at Buffalo Cave compared to the period either before or after, as seen at the Cave of Hearths and the Limeworks, respectively. This may be a significant factor in understanding the paleoenvironmental context of the Buffalo Cave deposit and the region as a whole.

Precise dating of the South African hominin sites has in the past been problematic beyond establishing broad faunal age ranges. Some success has been obtained from paleomagnetic dating at Sterkfontein, Makapansgat, Gondolin and Gladysvale (Herries, 2003) and at Kromdraii (Thackeray et al., 2002), but as yet well-confirmed absolute dating of these deposits has not been possible. At sites such as Sterkfontein many of the absolute dating methods so far applied have been contradictory. These problems, along with lack of large numbers of sites covering this time period, make it difficult to establish the relationship, if any, of climate change to hominine extinction or speciation during the early to middle Pleistocene in South Africa. It is therefore extremely important to better understand the stratigraphic, chronological and environmental context of early to middle Pleistocene sites such as Buffalo Cave.

## Conclusions

Primary paleomagnetic directions and their corresponding polarity zones were obtained from speleothem and clastic deposits from the fossil-rich Buffalo Cave, at Makapansgat, in the Limpopo Province of South Africa. Only parts of the flowstones were magnetically strong enough to be measurable. The clastic deposits were shown to contain ultrafine, magnetic oxide grains around the superparamagnetic to single-domain boundary range. The corresponding magnetically soft, viscous overprint was best removed by hybrid alternating field and thermal demagnetization. This enabled the isolation at low temperatures of a primary post-depositional remanent magnetization formed at, or close to, the time of deposition. By the combined use of paleomagnetism and faunal analysis it has been possible to construct a chronology for the Buffalo Cave deposits. By comparison with the Geomagnetic Polarity Time scale (GPTS) the whole sequence dates to between 1.95 Ma and 780,000 yr. The fossil-bearing deposits date to between 1.07 Ma and 780,000 yr, with the main layers dating to soon after 990,000 yr. This compares well with the faunal correlation dates between 1.0 Ma and 600,000 yr. The Buffalo Cave site is important because its paleontological record covers a period during the early to middle Pleistocene rarely represented elsewhere in southern Africa.

## Acknowledgments

The paleomagnetic and speleological work was funded by the Arts and Humanities Research Board (AHRB) Studentship No. 99/3050. The Variable Field Translation Balance (VFTB) used in this work was funded by NERC JREI grant GR3/E0069 to John Shaw, at the Geomagnetism Laboratory, University of Liverpool. This work was also undertaken with the support of the Makapansgat Research Advisory Committee at the University of the Witwatersrand, South Africa, the Palaeoanthropology Field School at Makapansgat (Institute of Human Origins and Arizona State University) and the Makapansgat Area Palaeoecology and Palaeoanthropology Project (MAPP). Permits to sample at Buffalo Cave held by K.L. Kuykendall were granted by the South African Heritage Resources Agency. Thanks to Darryl de Ruiter for helpful suggestions on an earlier version of the manuscript.

## References

Adams, J.W., Conroy, G.C., 2005. Plio-Pleistocene faunal remains from the Gondolin GD 2 in situ assemblage, North West Province, South Africa. In: Lieberman, D. (Ed.), Interpreting the Past: Essays on Human, Primate and Mammal Evolution. Brill Academic Publishers.

Behrensmeyer, A.K., Todd, N.E., Potts, R., McBrinn, G.E., 1997. Late Pliocene faunal turnover in the Turkana Basin, Kenya and Ethiopia. Science 278, 1589–1594.

Bosák, P., Pruner, P., Kalec, J., 2003. Magnetostratigraphy of cave sediments: applications and limits. Studia Geophysica and Geodaetica 47, 301–330.

Brennan, W.J., 1993. Origin and modification of magnetic fabric in fine-grained detrital sediment by depositional and post-depositional processes (SEPM Special Publication No. 49) Applications of Paleomagnetism to Sedimentary Geology 17–27.

Brink, J.S., 2002. Human fossil material discovered at Cornelia-Uitzoek. Culna 57, 4–7.

Broom, R., 1948. Some South African Pliocene and Pleistocene mammals. Annals of the Transvaal Museum 21, 1–38.

Curnoe, D., Grun, R., Taylor, L., Thackeray, J.F., 2001. Direct ESR dating of a Pliocene hominin from Swartkrans. Journal of Human Evolution 40, 379–391.

De Ruiter, D.J., 2003. Revised faunal lists of members 1–3 of Swartkrans, South Africa. Annals of the Transvaal Museum 40, 29–41.

Fisher, R., 1953. Dispersion on a sphere. Philosophical Transactions of the Royal Society of London A, vol. 306, pp. 295–305.

Grun, R., Brink, J.S., Spooner, N.A., Taylor, L., Stringer, C.B., Franciscus, R.G., Murray, A.S., 1996. Direct dating of the Florisbad hominid. Nature 382, 500–501.

Herries, A.I.R., 2003. Magnetostratigraphic seriation of South African hominin palaeocaves. Ph.D Thesis, Geomagnetism Laboratory, Department of Archaeology, University of Liverpool.

Herries, A.I.R, Latham, A.G., Kuykendall, K.L., 2001. The use of 'SRT' in sampling the Makapansgat Limeworks hominid palaeocave, South Africa. Antiquity 75, 251–252.

Herries, A.I.R., Adams, J.W., Kuykendall, K.L., Shaw, J., in Press. Speleology and magnetobiostratigraphic chronology of the Gondolin hominin palaeocave, S. Africa. J. Human Evolution.

Hopley, P., 2004. Palaeoenvironmental reconstruction of South African hominin-bearing cave deposits using stable isotope geochemistry. PhD Thesis. Department of Earth Sciences and Archaeology, University of Liverpool.

Kirschvink, J.L., 1980. The least-square line and plane and the analysis of palaeomagnetic data. Geophysics. Journal of the Royal Astronomical Society 62, 699–718.

Klein, R.G., 1977. The ecology of early man in South Africa. Science 197, 115–126.

Kuykendall, K.L., Toich, C.A., McKee, J.K., 1995. Preliminary analysis of the fauna from Buffalo Cave, Northern Transvaal, South Africa. Palaeontologia Africana 32, 27–31.

Lacruz, R.S, Brink, J.S., Hancox, J., Skinner, A.S., Herries, A., Schmidt, P., Berger, L.R., 2002. Palaeontology and geological context of a middle Pleistocene faunal assemblage from the Gladysvale Cave, South Africa. Palaeontologia Africana 38, 99–114.

Latham, A.G., Ford, D., 1993. The palaeomagnetism and rock magnetism of cave and karst deposits (SEPM Special Publication No. 49) Applications of Paleomagnetism to Sedimentary Geology 149–155.

Maguire, J., 1998. Makapansgat: a guide to the palaeontological and archaeological sites of the Makapansgat Valley. The Dual Congress of the International Association for the Study of Human Palaeontology and International Association of Human Biologists. Sun City, Republic of South Africa.

Ogg, J.G., Smith, A.G., 2004. The geomagnetic polarity timescale. In: Gradstein, F., Ogg, J., Smith, A. (Eds.), A Geologic Time Scale. Cambridge University, pp. 63–86.

Schoenwetter, J., 2000. Makapansgat and Buffalo Cave Palynology: a brief assessment of studies during Spring 1999. In: Kuykendall, K.L. (Ed.), Palaeoecological Investigations in the Makapansgat Valley, Northern Province, South Africa. Report submitted to the Makapansgat Research Advisory Committee, BPI.

Thackeray, J.F., Watson, V., 1994. A preliminary account of faunal remains from Plovers Lake. South African Journal of Science 90, 231–232.

Thackeray, J.F., Kirschvink, J.L, Raub, T.D., 2002. Palaeomagnetic analysis of calcified deposits from the Plio-Pleistocene hominid site of Kromdraai, South Africa. South African Journal of Science 98, 537–540.

Tobias, P.V., 1971. Human skeletal remains from the Cave of Hearths, Makapansgat, Northern Transvaal. American Journal of Physical Anthropology 34, 335–367.

Tobias, P.V., 1997. Some little known chapters in the early history of the Makapansgat fossil hominid site. Palaeontologia Africana 33, 67–79.

Vrba, E.S., 1995. The fossil record of African antelopes (Mammalia, Bovidae) in relations to human evolution and paleoclimate. In: Vrba, E. S., Denton, G.H., Partridge, T.C., Burckle, L.H. (Eds.), Paleoclimate and Evolution with Emphasis on Human Origins. Yale University Press, New Haven, pp. 385–424.

Wood, B., 1999. Plio-Pleistocene hominins from the Baringo Region, Kenya. In: Andrews, P., Banham, P. (Eds.), Late Cenozoic Environments and Hominid Evolution: A Tribute to Bill Bishop. Geological Society, London, pp. 113–122.